Environment International 130 (2019) 104883

Contents lists available at ScienceDirect

Environment International

journal homepage: www.elsevier.com/locate/envint

Population and single cell metabolic activity of UV-induced VBNC bacteria determined by CTC-FCM and D_2O-labeled Raman spectroscopy

Lizheng Guo[a,b], Chengsong Ye[a], Li Cui[a], Kun Wan[a,b], Sheng Chen[a,b], Shenghua Zhang[a,*], Xin Yu[a,*]

[a] Key Lab of Urban Environment and Health, Institute of Urban Environment, Chinese Academy of Sciences, Xiamen 361021, China
[b] University of Chinese Academy of Sciences, Beijing 100049, PR China

ARTICLE INFO

Handling Editor: Frederic Coulon

Keywords:
Viable but non-culturable
UV disinfection
CTC-FCM
D_2O-labeled Raman
Respiration activity
Metabolic activity

ABSTRACT

The occurrence of viable but non-culturable (VBNC) bacteria will result in significant underestimation of viable bacterial counts in drinking water. Whereas, much is unknown in characterizing their viability. In this study, two environmental isolates (*Aeromonas* sp. and *Pseudomonas* sp.) and two model strains (*E. coli* and *S. aureus*) were induced into VBNC state by UV irradiation. Then, their metabolic activity was determined by 5-cyano-2,3-ditolyl tetrazolium chloride combination flow cytometry (CTC-FCM) and D_2O-labeled Raman spectroscopy, respectively, at both population and single cell levels. The results showed that almost all strains could enter VBNC state irradiated by ≥ 5 mJ/cm^2 UV. When determined by CTC-FCM, the population metabolic activity for each strain did not vary significantly ($p > 0.05$) unless the UV dose reached 200 mJ/cm^2. Their single cell activity spectrum narrowed slightly, as indicated by changes in the standard deviation of the logarithmic normal distribution (σ) of 0.015–0.033. This minute difference suggested the CTC-FCM method was suitable for assessing the essential viability of VBNC bacteria. With respect to Raman method, an obvious dose-response effect was recorded. With the UV dosages increased from 10 to 200 mJ/cm^2, the CD/(CD + CH) for the four strains were reduced to between 95.7% and 47.9% of unirradiated controls, depending on strain and UV dose. Meanwhile, the single cellular Raman spectrum showed much more heterogeneously metabolic activity distribution, with some cells even entering metabolic "silence". Considering the ubiquitous participation of water in biochemical processes, the Raman method was more appropriate in assessing the overall metabolic activity. The above findings can not only be a reference for VBNC mechanism studies, but also have the potential in optimizing disinfection and other bacterial removal processes.

1. Introduction

Viable but nonculturable (VBNC) bacteria in the environment have received widespread attention (Oliver, 2005; Oliver, 2010; Ramamurthy et al., 2014) ever since Xu et al. first identified the VBNC state in *Escherichia coli* and *Vibrio cholera* (Huai-Shu et al., 1982). Because VBNC bacteria have lost culturability (i.e. the ability to form colonies on general culture media), they are difficult to detect and their presence in drinking water is therefore often significantly underestimated (Oliver, 2000). The presence of VBNC bacteria in drinking water can threaten water quality and public health (Bedard et al., 2014; Dietersdorfer et al., 2018; Whitesides and Oliver, 1997). Many disinfectants used to prevent the spread of pathogenic microorganisms can induce a VBNC state, including ozone (Orta de Velasquez et al., 2017) , chlorine, and chloramine (Chen et al., 2018; Liu et al., 2010). Increasing research on ultraviolet (UV) disinfection has revealed that it may induce the VBNC state and that bacteria could resuscitate under favorable growth conditions (Ben Said et al., 2010; Zhang et al., 2015). Some advantages of UV disinfection include cost-effectiveness, an absence of treatment by-products, and high sterilization efficiency against *Cryptosporidium parvum* oocysts and *Giardia lamblia* cysts (Belosevic et al., 2001). Therefore, as an emerging technology, UV disinfection has been widely applied in small drinking water treatment plants (DWTPs), as well as reclaimed and wastewater treatment plants. Although UV disinfection has many advantages, its effectiveness as a method for permanently inactivating bacteria remains controversial (Guo and Kong, 2019; Guo et al., 2012; Zhang et al., 2015). And little is known about the physiological characteristics of VBNC bacteria induced by UV irradiation.

Unfortunately, most studies on VBNC bacteria have focused on model or indicator strains rather than on environmental bacteria. Experimental data on model strains cannot be directly applied to

* Corresponding authors.
E-mail addresses: shzhang@iue.ac.cn (S. Zhang), xyu@iue.ac.cn (X. Yu).

https://doi.org/10.1016/j.envint.2019.05.077
Received 10 March 2019; Received in revised form 19 May 2019; Accepted 30 May 2019
Available online 21 June 2019

environmental strains, even when the classification, growth conditions, nutrition characteristics, and genetic information of the strains are clearly known. On the one hand, it is still unclear whether model strains can stably exist in the environment. And on the other hand, model strains inadequately represent the complex assemblage of strains found in environmental communities (Santos et al., 2013). Thus, it is necessary to carry out studies on bacteria isolated from the environment. The information gained from studying environmental isolates may provide clues to understanding the effects of environmental stress on inducing bacteria into a VBNC state, as well as the means by which natural microorganisms survive and resist harsh environments.

One of the most critical issues in studying VBNC bacteria is determining residual viability. VBNC bacterial frequently display high ATP production (Lindback et al., 2010), continuous gene expression (Trevors, 2011), respiration activity (Chen et al., 2018; Lin et al., 2017), and metabolic activity (Rahman et al., 1994; Tholozan et al., 1999), all of which are associated with normal metabolism, pathogenic maintenance, and resuscitation. Some studies have used the PMA-qPCR method to detect the viability of bacteria based on membrane integrity (Ge et al., 2019; Lee and Bae, 2018; Mangiaterra et al., 2018). And other studies have used 5-cyano-2, 3-ditolyl tetrazolium chloride and flow cytometry (CTC-FCM) to detect bacterial respiration (Chen et al., 2018; Lin et al., 2017) because the technique is fast and easy to manipulate (Wilkinson, 2018). CTC is a soluble tetrazolium salt that can penetrate into cell membranes where it is reduced to insoluble, intracellular formazan crystals which can then be detected using flow cytometry (Wilkinson, 2018). However, previous studies have not evaluated the degree to which CTC-FCM can characterize actual bacteria activity. A detailed and in-depth analysis of CTC-FCM may enable a clearer understanding of the activity characteristics of bacterial populations as well as the range of applications of this method.

Another approach for determining the metabolic activity of VBNC bacteria involves measuring the uptake of substrates, such as glucose, $(NH_4)_2SO_4$ (Zeng et al., 2013), and methionine (Rahman et al., 1994). However, the substrate uptake method is time consuming (Rahman et al., 1994) and can only detect the average activity of bacteria at the population level. It is well known that the activity of individual cells differs even within the same system (Smith and Giorgio, 2003). Therefore, here we try to use a rapid and nondestructive method, D_2O-labeled Raman spectroscopy, to detect the metabolic activity of VBNC bacteria at the single-cell level. H_2O is heavily involved in cellular metabolic activities, including the synthesis of fatty acids, proteins, and nucleic acids (Justice et al., 2014; Valentine et al., 2004; Ye et al., 2017a; Zhang et al., 2009). The deuterium isotope of hydrogen can substitute hydrogen in water (D_2O) and form C-D bonds during fatty acid and protein synthesis. Raman spectroscopy can provide a comprehensive intracellular molecular spectrum based on the vibration frequencies of characteristic chemical bonds (Berry et al., 2015; Song et al., 2017; Zhang et al., 2018). For example, Chen et al. used this method to identify cells with metabolic activity after treatment with 4 mg/L chlorine (Chen et al., 2018). In this study, D_2O-labeled Raman method was used to quantify the metabolic activity of VBNC bacteria on a single cell level after UV disinfection.

At present, most studies on VBNC bacteria are focused on induction conditions, detection methods, resuscitation environment (Ramamurthy et al., 2014), and infectivity (Dietersdorfer et al., 2018; Pianetti et al., 2012). However, an in-depth analysis of the activity characteristics of bacteria in that state is still lacking. In this study, two common opportunistic pathogens isolated from an aquatic environment, *Aeromonas* sp. and *Pseudomonas* sp., and two model strains Gram-negative *E. coli* CMCC 44103 and Gram-positive *S. aureus* ATCC 6538 were induced into VBNC state by UV irradiation. Two methods, i.e. CTC-FCM and D_2O-labeled Raman Spectroscopy, were used to assess the viability/activity of the VBNC bacteria. It was expected that both population and single cell level metabolic activity could be elucidated from different angles. We believe this work provides support for the development of effective strategies for mitigating potential risks from VBNC strains in drinking water.

2. Materials and methods

2.1. Environmental and model strains

Environmental strains were isolated from the secondary effluent of a wastewater treatment plant in Xiamen, China. The water samples were collected in March, April, and May 2017. The samples were immediately transported to the lab and stored at 4 °C. The heterotrophic plate count (HPC) method was used to acquire bacteria colonies culturable in water. Colonies recovered from the plates were selected for further isolation and purification. DNA was extracted by adding single colonies to 50 μL lysis buffer (TaKaRa, Cat. #: 9164, Japan) and then following the manufacturer's protocol: incubation at 85 °C for 15 min, light centrifugation, and then PCR amplification of 2 μL supernatant. The genus level of the isolated bacteria was identified by PCR amplification of the 16S ribosomal RNA gene. The primers used in the study were: 27F, 5′-AGAGTTTGATCMTGGCTCAG-3′ and 1492R, 5′-TACGGT TACCTTGTTACGACTT-3′ (Suzuki and Giovannoni, 1996). The PCR products were sent to Majorbio (Location, China) for purifying and sequencing. The sequences obtained were submitted to NCBI for alignment with the GenBank database (http://www.ncbi.nlm.nih.gov/blast). Based on the results, opportunistic pathogens that appeared at all three sampling times, i.e. *Aeromonas* sp. and *Pseudomonas* sp., were selected. Strains were frozen in 25% glycerin at −80 °C until use.

Two model strains, *E. coli* CMCC 44103 and *S. aureus* ATCC 6538, were bought from Guangdong Microbial Culture Collection Center (GDMCC, China) and Marine Culture Collection of China, respectively.

2.2. Strain growth conditions and UV disinfection

All of the four above strains were incubated in Luria-Bertani (LB) broth (Hopebio, China) at 37 °C on a 150-rpm shaking incubator overnight to ensure that the bacteria concentration reached 10^9 CFU/mL, as confirmed by a standard plate count on nutritional agar (NA) (Hopebio, China) incubated at 37 °C for 24 h. Cultures were harvested by centrifugation at 9000*g* for 10 min and washed twice with 0.9% sodium chloride solution. Samples were resuspended and then diluted to approximately 10^6 CFU·mL^{-1} in 0.9% sodium chloride solution in preparation for UV irradiation.

The irradiation experiment was performed using a collimated beam apparatus that contained a low-pressure (15 W) mercury UV-C lamp (254 nm, Philips, USA) (Zhang et al., 2015). The UV lamp was housed above a collimating tube (46 cm) which aids in focusing the UV beam. The UV intensity (0.12 mW/cm^2) was measured by a radiometer (TRINR TN-2254, Taiwan) and corrected according to the method by Bolton and Linden (Bolton and Linden, 2003). The UV dose (mJ/cm^2) was calculated by multiplying UV intensity (mW/cm^2) by sample exposure time (seconds). A petri dish containing 20 mL bacterial suspension was placed horizontally below the collimating tube and a magnetic stirring bar was used to homogenize the suspension during irradiation. The UV doses applied in this work were 0, 3, 5, 10, 15, 25, 50, 100, 200, or 800 mJ/cm^2.

2.3. Culturable, viable, and total bacteria counts and detection of CTC-FCM activity (respiration intensity)

The HPC method was used to detect the number of culturable bacteria before and after UV irradiation. Aliquots of the bacteria suspension were plated onto NA with ten-fold dilution and cultured at 37 °C in the dark for 24 h. Viable and total bacteria were detected by CTC staining (Thermo Fisher, USA) and enumerated by flow cytometry (Millipore Guava EasyCyte, USA). Eight microliters of CTC stock solution were added to 192 μL bacteria suspension for a final concentration

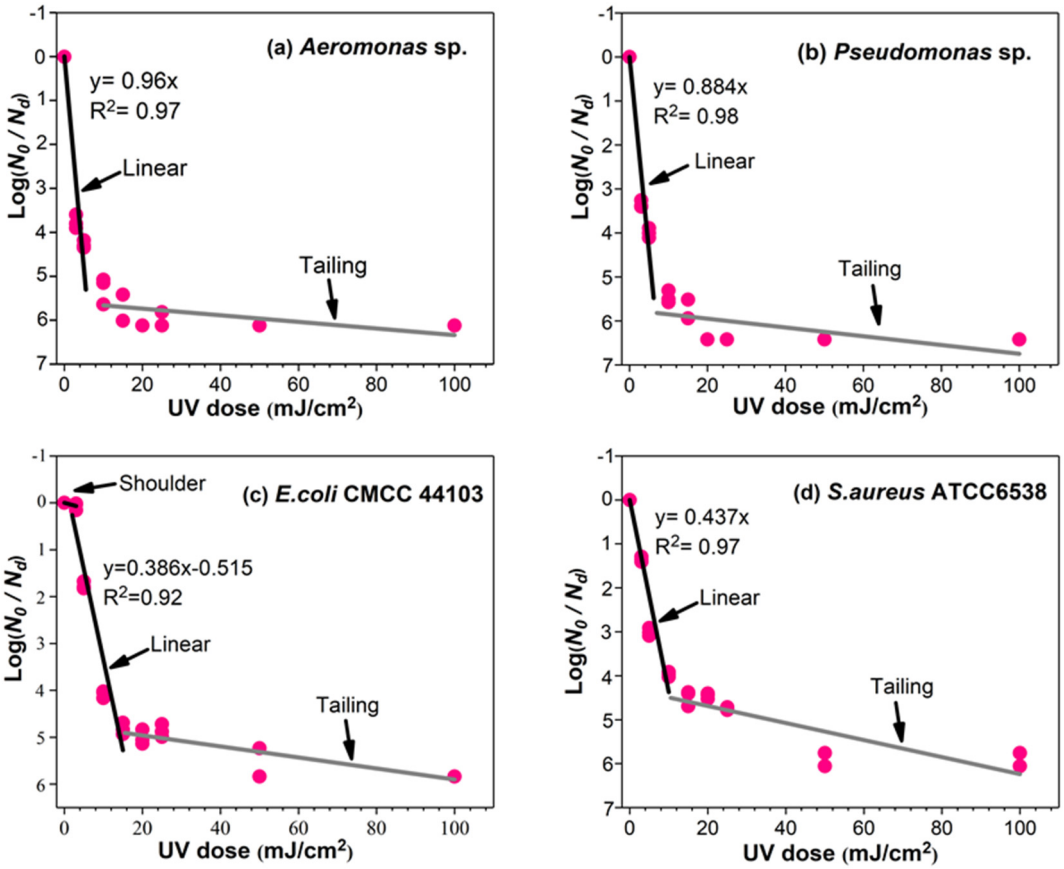

Fig. 1. Ultraviolet fluence-response curves for isolated and model strains. Each circle represents the average of three parallel. And three replicates have been done. Regression analysis and 95% confidence interval (CI) were carried out on the data used to fit the linear sections.

of 2 mmol/L. Samples were incubated at 37 °C for 4 h in the dark and then measured on a FCM (Gernsheim, Germany) or a FlowSight® imaging flow cytometer (Amnis®, part of EMD Millipore, Germany). Cell-free and killed controls were run to check for abiotic reduction to formazan. CTC fluorescence intensity was acquired during flow cytometry (Lin et al., 2017) and the average respiration intensity of the cells was characterized using the average fluorescence intensity. In order to investigate the distribution of respiration intensity of the bacterial strains, we drew a logarithmic normal distribution map N (μ, σ^2) based on fluorescence intensity.

2.4. Detection of VBNC metabolic activity using D_2O labeled Raman spectroscopy

We first tested the sensitivities of the isolated and model strains to D_2O solution. Five microliters of stationary phase cultures were inoculated into 5 mL LB broth containing 0, 5, 10, 20, 30, 40, or 60% heavy water (D_2O, 99.9% atom% D, Macklin, China). Next, 200 μL aliquots were transferred into a 96-well plate. Bacterial growth was monitored every 20 min using a microplate reader (SpectraMax 190, USA) at 600 nm (OD600).

After UV irradiation, the treated bacterial solutions were transferred into LB broth to reach a final D_2O concentration of 25% or 30%. The D_2O-containing tubes were incubated at 37 °C on a 150 rpm shaking incubator and sampled at 0, 10, 20, 30, 40, and 60 min for Raman spectroscopy. The harvested cells were washed twice by centrifugation at 5000 rpm for 3 min using sterile water to eliminate the impact of the culture medium. Aliquots of 2 μL of the prepared bacteria were dispersed on aluminum-coated substrates and air-dried before Raman analysis (Cui et al., 2018). Single microbial cell Raman spectra ranging from 500 to 3300 cm^{-1} were obtained using a LabRAM ARAMIS (Horiba, Japan) confocal micro-Raman system equipped with a 532 nm Nd: YAG excitation laser and a 300 grooves/mm grating (Cui et al., 2018). A 100× magnifying dry objective (NA = 0.90, Olympus) was used to observe and collect the Raman signal. All cells were detected randomly. The integrated spectral intensities of the C-D band (2040–2300 cm^{-1}) and the C—H band (2800–3100 cm^{-1}) were used to quantify the degree of D substitution in C—H bonds (C-D ratio), i.e. bacterial metabolic activity was expressed as C-D/(C-D + C-H) (Tao et al., 2017).

2.5. Analytical methods

The UV sensitivity of bacteria is described by the parameters of their inactivated kinetics. The first-order disinfection model of Chick and Watson (Eq. (1)), which related to chemical disinfection, can also be applied to UV disinfection (Hijnen et al., 2006; Mamane-Gravetz and Linden, 2005).

$$N_t = N_0 \cdot e^{-kt} \quad (1)$$

The linear curves are described by the following formula:

$$\mathrm{Log10}\frac{N_0}{N_t} = k \cdot H \quad (2)$$

where N_0 is the initial bacteria concentration (CFU/mL) before exposure to UV irradiation; N_t is the bacteria concentration after contact time t. The Log_{10} transformation for N_0/N_t and UV fluence (H) determined the inactivation rate constant k (cm^2/mJ) from the linear section. A high k value signifies that bacteria are more sensitive to UV irradiation.

Results in this work are represented as means ± standard deviation (SD). Significant differences between viable bacteria were tested using a

one-way analysis of variance (ANOVA). $p < 0.05$ was considered significant. Statistical analyses were performed using SPSS 16.0 (IBM, USA).

3. Results

3.1. Impacts of UV treatment on the culturability of environmental and model strains

Fig. 1 shows the linear fit of the four bacterial strains as a function of UV fluence. A high coefficient was observed between low UV exposure and the log inactivation of bacteria. A tailing zone appeared after the first order reaction zone as UV dose increased, demonstrating that culturable bacteria persist even at a UV fluence of 100 mJ/cm^2. For the two environmental isolates, the k values were 0.960 cm^2/mJ and 0.884 cm^2/mJ, which were higher than *E. coli* (k = 0.386 cm^2/mJ) and *S. aureus* (0.437 cm^2/mJ) (Fig. 1a and b), illustrating that the environmental strains were more sensitive to UV irradiation than the model strains. There was 3–4-log inactivation at the 3 mJ/cm^2 UV dose, as shown in Fig. 1a and b.

For *E. coli*, a "shoulder" was observed at UV doses ranging from 0 to 3 mJ/cm^2 (Fig. 1c). But there were still 5-log removals under normal drinking water disinfection doses (20–40 mJ/cm^2). *S. aureus*, as a Gram-positive bacterium, did not exhibit a higher resistance to UV irradiation than *E. coli* (Fig. 1d). Its log inactivation curves were similar to the log survival curves reported by Chang et al. in which 4-log inactivation was also observed at a 10 mJ/cm^2 UV dose (Chang et al., 1985).

3.2. Occurrence of VBNC bacterial cells after UV irradiation

After UV irradiation, the number of VBNC bacterial cells for all four strains was calculated as the difference between the number of viable and culturable cells. Fig. 2 shows the number of total, viable, and culturable cells after UV treatment using the CTC-FCM and HPC methods. No significant differences ($p > 0.05$) were observed in the viable cell number when the UV dose was below 200 mJ/cm^2. Even when the UV fluence was increased to 800 mJ/cm^2, there was only an approximately one-log unit drop in the number of viable cells for the four bacterial strains. The ratio of culturable to viable cells showed a substantial decrease with increasing UV dose (Fig. 2e), indicating that most of the culturable bacteria were converted to VBNC bacteria as UV dose increased. With the increase in UV dose from 50 to 800 mJ/cm^2, almost all viable bacterial cells entered a VBNC state (Fig. 2a-d).

3.3. Respiration intensity of VBNC bacteria under different UV doses

Fig. 3A shows the average respiration intensity of the four VBNC bacterial strains under various UV fluences. No significant differences ($p > 0.05$) were detected between the control group and the treatment groups when the UV dose was below 50 mJ/cm^2. The respiration intensity of all strains except for *S. aureus* decreased at UV doses under 200 mJ/cm^2. Overall, the respiratory intensities of the four strains remained high under UV doses applicable in DWTPs compared with the unirradiated group (Fig. 3A). The respiratory activities determined by the CTC-FCM method displayed a dose-independent effect under low UV fluence.

Fig. 3B presents the distribution of respiration intensity of the bacterial strains based on single cells grouping. The results illustrate that respiratory intensity conformed to the logarithmic normal distribution even with high UV dose irradiation. With increasing UV fluence, the distribution range, expressed in terms of standard deviation (σ value: *Aeromonas* sp., 0.320 to 0.287; *Pseudomonas* sp., 0.300 to 0.285; *E. coli*, 0.360 to 0.337; *S. aureus*, 0.438 to 0.414), narrowed slightly. A smaller σ value indicated that the distribution was more centered around the average value and that the heterogeneity of respiration intensity in the population was low.

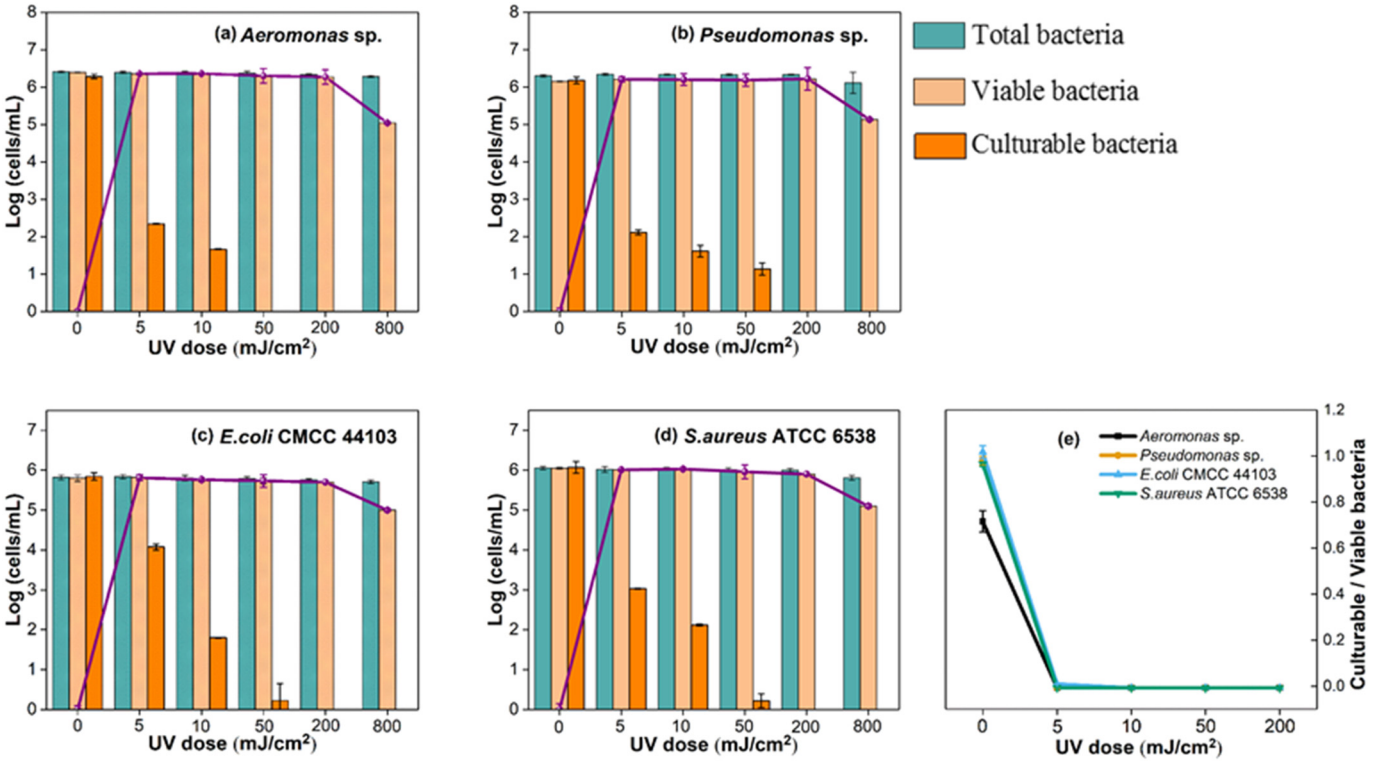

Fig. 2. Total, viable, and culturable cell counts of isolated and model strains after treatment by various UV fluences. The purple line represents the number of VBNC bacteria, determined as the difference between the number of viable and culturable cells. (e) The ratio of culturable to viable bacterial cells with increasing UV dose. (For interpretation of the references to color in this figure legend, the reader is referred to the web version of this article.)

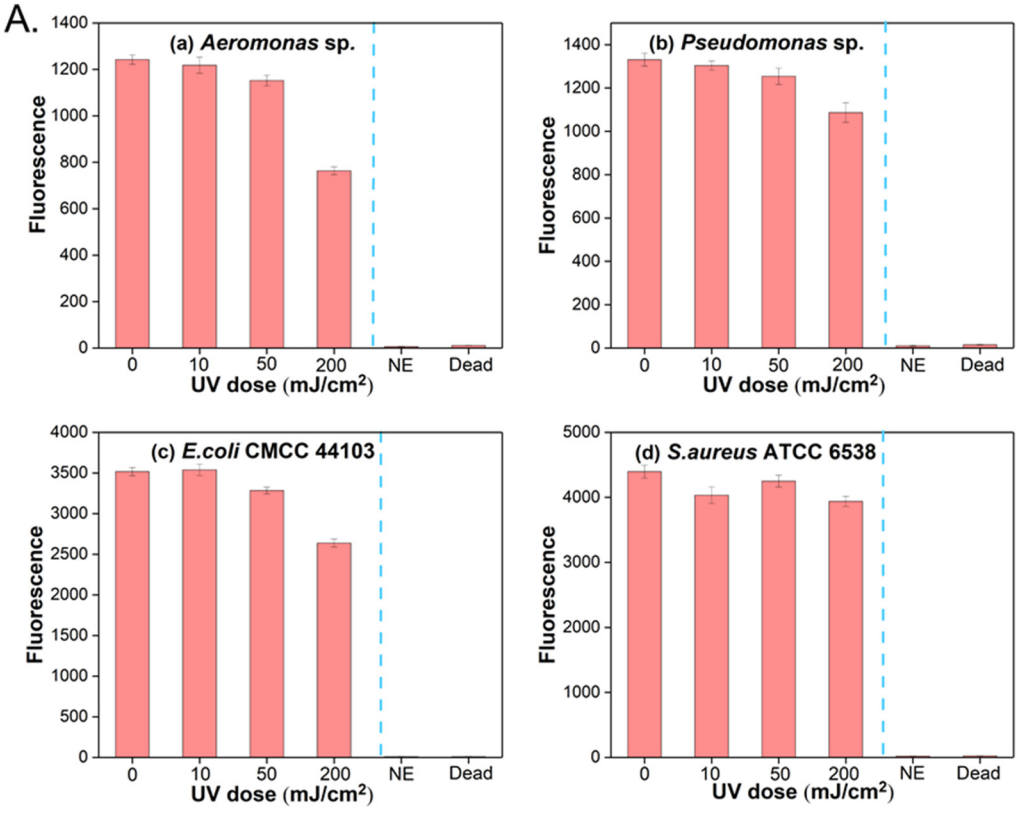

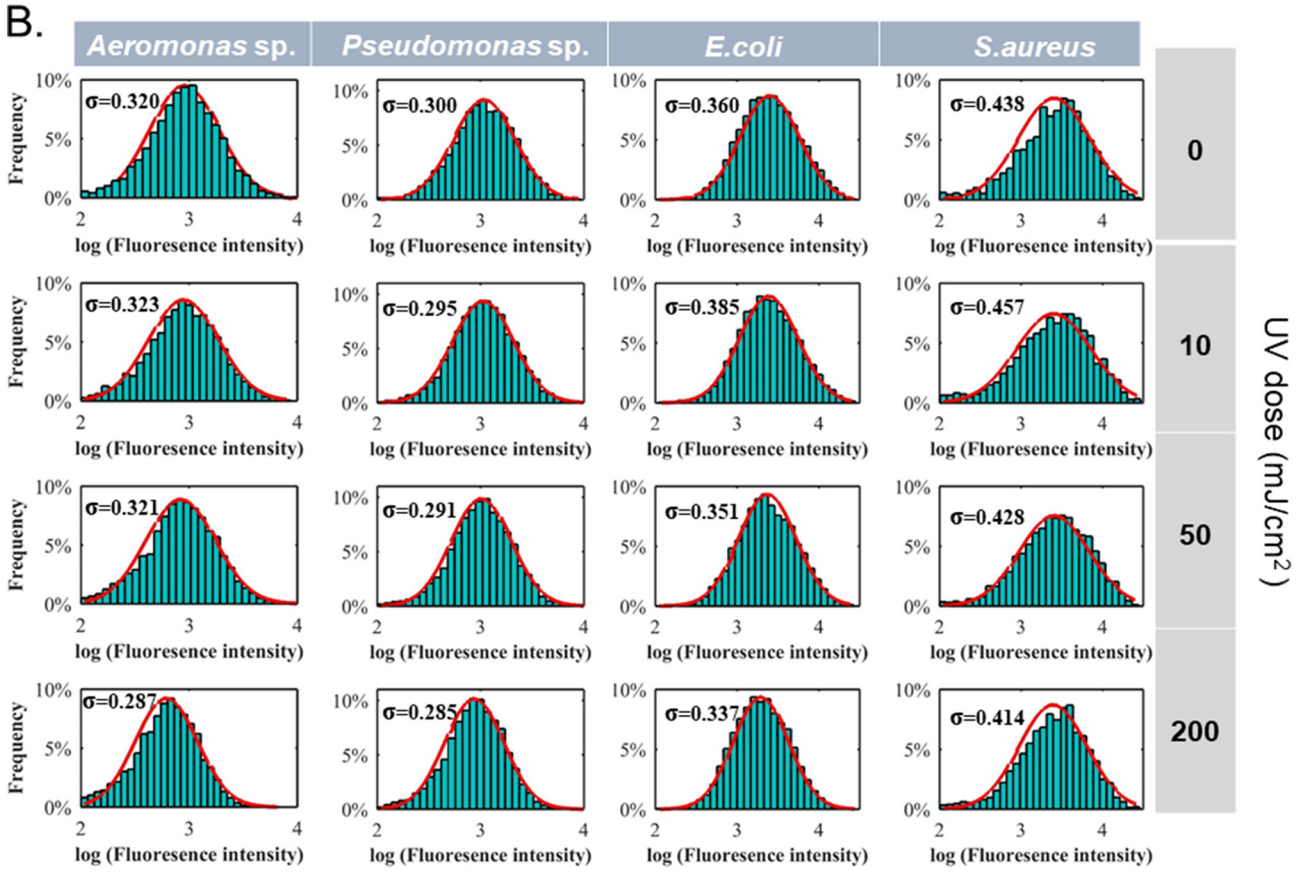

(caption on next page)

Fig. 3. A. Average respiration intensity of individual cells under various UV doses for the four tested bacterial strains. "NE" represents the negative control (cell-free) and "Dead" represents a control containing bacteria killed by boiling in water for 30 min; B. Respiratory intensity distribution of the four bacterial strains under different UV fluences. The red line represents the logarithmic normal distribution curve for each population. σ represents the standard deviation of logarithmic normal distribution. (For interpretation of the references to color in this figure legend, the reader is referred to the web version of this article.)

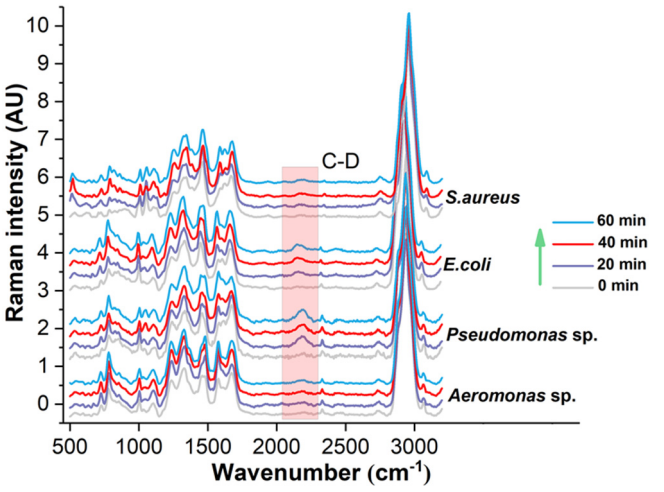

Fig. 4. Gradual emergence of the C-D peak in the SCRS of the four bacterial strains under 30% (v/v) or 25% (v/v) (for *Aeromonas* sp.) D_2O. Each spectrum represents the average of 20 cells.

3.4. Metabolic activity in VBNC bacteria determined by single-cell D_2O-labeled Raman spectroscopy

3.4.1. Tracking heavy water incorporation in active environmental and model strains via Raman microspectroscopy

The effect of different heavy water concentrations on bacterial growth is shown in Fig. S1. Compared with the D_2O-free control for each strain, *Aeromonas* sp. was sensitive to D_2O, exhibiting a slight inhibition in growth with 30% (v/v) heavy water (Fig. S1a). Meanwhile, 40% (v/v) heavy water had no significant effects on the growth of *Pseudomonas* sp. or *S. aureus* (Fig. S1b and S1d). *E. coli* tolerated the highest levels of D_2O (up to 60%) (Fig. S1c).

A broad C-D Raman band in the 2040 to 2300 cm^{-1} region appeared in single-cell Raman spectra (SCRS) for the tested bacterial strains due to a Raman shift of the original C—H peak (2800 to 3100 cm^{-1}) (Fig. 4). The C-D peak appeared rapidly and could be detected within 20 min after the start of incubation, which allowed timely monitoring of metabolic activity in single cells. At D_2O concentrations below 30% (v/v) (25% (v/v) for *Aeromonas* sp.), bacterial growth was unaffected (almost equivalent to the blank control) and a dynamic C-D band was produced which increased significantly with increasing culture time, allowing intensity changes in the C-D band at different culture times to be quantified. Therefore, 30% (v/v) heavy water (25% (v/v) for *Aeromonas* sp.) was selected to detect changes in bacterial

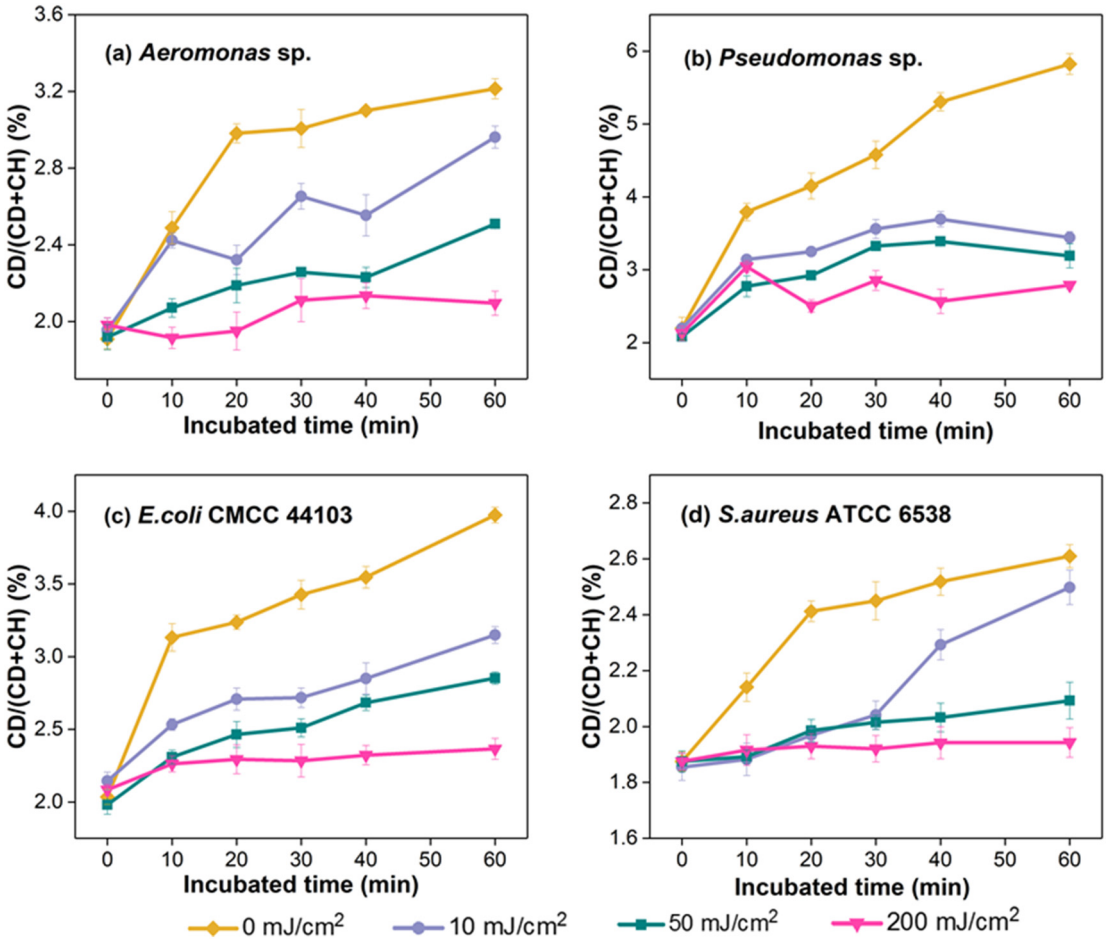

Fig. 5. Temporal dynamics of C-D ratios of the four bacterial strains with increasing UV dose. Each point represents the C-D ratio for 20 cells with three replicates.

metabolic activity after irradiation by different UV fluences.

3.4.2. Quantitative characterization of VBNC metabolic activity

The four strains tested in this work were able to actively take up heavy water and the emergence of C-D bands was significant. Therefore, CD/(CD + CH) was used to model the metabolic activity of VBNC bacteria. After 10 mJ/cm^2 UV irradiation, the number of culturable bacterial cells was less than one ten-thousandth of the number of viable bacteria (Fig. 2), indicating that the probability that culturable bacteria were detected during Raman detection was extremely small. Therefore, we concluded that the detected bacteria were nearly all VBNC bacteria. The duration of metabolic activity detection was limited to 1 h of incubation to reduce the possibility of bacterial regrowth caused by the "tailing" phenomenon of UV disinfection.

The absorption of heavy water by bacteria goes through a logarithmic phase and then plateaus with a saturated C-D ratio. However, when bacterial metabolic activity is inhibited, the absorption of heavy water lags (Tao et al., 2017). The temporal dynamics of C-D ratios under various UV fluences are shown in Fig. 5. At 0 mJ/cm^2 UV irradiation, the C-D ratios of the four bacterial strains initially increased rapidly and then continued to rise at a much slower rate. When the UV dose ranged from 10 to 200 mJ/cm^2, the metabolic activity of VBNC *Aeromonas* sp. was reduced to 92.1–65.2% of the activity of the unirradiated control. Similarly, the activities were 59.1–47.9% for *Pseudomonas* sp., 79.2–59.5% for *E. coli*, and 95.7–74.5% for *S. aureus* (Fig. 5a, b, c, d).

Moreover, the C-D ratios of the four strains showed large difference. For *Aeromonas* sp. and *S. aureus* treated with 10 mJ/cm^2 UV (Fig. 5a and d), the C-D ratios reached nearly the same levels as those of the unirradiated controls after 1 h of incubation. In contrast, *Pseudomonas* sp. and *E. coli* experienced significant reductions (Fig. 5b and c). The C-D ratio of *Pseudomonas* sp. reached saturation after 30 min of incubation at all levels of UV irradiation (Fig. 5b), indicating that its absorption and metabolism of water had reached equilibrium. At the highest UV dose (200 mJ/cm^2), the C-D ratios of the four strains were at a comparably low level after they reached saturation within 1 h.

Single cell activities were also measured using D_2O-labeled Raman. The difference between the C-D ratio of single cells at a specific time point and the average C-D ratio at 0 min incubation was defined as the ΔC-D ratio. A ΔC-D ratio below zero was considered to represent a metabolic state of "silence" (Tao et al., 2017). The metabolic activities of each single cell and the distribution of the whole population are shown in Fig. 6. The results revealed that a higher UV dose generally resulted in a lower metabolic heterogeneity. For example, the ΔC-D ratio for *Aeromonas* sp. was much higher at 10 mJ/cm^2 UV irradiation (0.0105 ± 0.0071) than at 50 mJ/cm^2 (0.0060 ± 0.0061) and likewise for *E. coli* (0.0109 ± 0.0076 and 0.0079 ± 0.0056, respectively). At a high UV dose of 200 mJ/cm^2, most bacterial cells maintained metabolic activity and only a small portion entered metabolic "silence".

4. Discussion

4.1. The effect of UV disinfection on inducing a VBNC state in environmental and model strains

UV disinfection has been increasingly applied in water treatment processes because it produces few toxic byproducts and can effectively inactive a wide variety of pathogens (Belosevic et al., 2001; Lee et al., 2015). However, doubts remain about the fate of UV irradiated bacteria due to photoreactivation (Guo et al., 2012) and the occurrence of VBNC bacteria (Zhang et al., 2015). In the current study, we demonstrate that both environmental and model strains can be induced into a VBNC state. At UV doses between 5 and 200 mJ/cm^2, the majority of cells lost culturability but remained viable (Fig. 2). This demonstrates that environmental bacteria induced into the VBNC state may maintain partial biological activity even after UV disinfection in full-scale drinking water treatment processes. In addition, environmental and model strains showed different responses to UV irradiation in terms of culturability and metabolic activity. For example, even though *Aeromonas* sp. was more sensitive than *E. coli* to UV irradiation as detected by the HPC method (Fig. 1), this environmental strain maintained higher metabolic activity (Fig. 5). Further study on isolated strains may enable a more complete understanding of UV resistance in environmental bacteria. VBNC bacteria decrease the reliability of UV irradiation-based bacterial disinfection processes, which may pose a health risk when these bacteria reach the point of use. Therefore, in order to accurately assess health risks from drinking water after disinfection, especially from pathogens that maintain virulence in the VBNC state or can resuscitate in a host, detection methods must combine current cultivation methods with improved methods for detecting microbial metabolic activity (Albrecht et al., 2007).

4.2. CTC-FCM effectively characterized the essential viability of VBNC bacteria

CTC-FCM has been used to detect the respiratory activity of bacteria at different pressures (Chen et al., 2018; Zhang et al., 2018) and in different environmental systems (Servais et al., 2001). Even though CTC-FCM is a rapid and convenient method for determining the activity of cells, the question remains how well it reflects the actual activity of bacteria. The CTC-FCM results in the current study suggest that UV exposure had little effect on bacterial respiration (Fig. 3A) and the distribution of respiration intensity in a population (Fig. 3B). Electron transfer is an essential physiological process in viable cells and depends on the availability of an energy source or retained enzyme activity (Kell et al., 1998). CTC is reduced prior to ubiquinone in the respiratory chain by primary aerobic [succinate and NAD(P)H] dehydrogenases (Smith and McFeters, 1997), which indicates that CTC is only involved in portion of the respiratory activity and therefore fluorescence intensity perhaps more precisely reflects only the redox ability of the electron transport chain. Specific oxygen uptake rate (SOUR) is another method for measuring the respiration activity of bacteria and is based on oxygen consumption. Lin et al. reported a lower respiration rate of VBNC bacteria using the SOUR method compared with the CTC-FCM method (Lin et al., 2017). Based on these, we conclude that the CTC-FCM method does not well-reflect the overall activity of bacteria. Rather, CTC-FCM detects only the essential viability of bacteria necessary to keep cells alive after UV disinfection.

In this study, we did not observe a significant decrease in bacterial respiration activity with increasing UV dose (Fig. 3A). In contrast, a significantly lower bacterial respiration intensity has been observed with increasing doses of other disinfectants such as chlorine (Chen et al., 2018). These differences may be due to the different mechanisms these disinfectants use to inactivate/kill the bacteria. UV-C light targets nucleic acids (Nocker et al., 2007) but not the cell membrane where the respiratory electron transport chain is located, whereas chlorine disinfection damages cell membrane integrity (Chen et al., 2018). An intact cell membrane ensures the integrity of the electron transport chain and the normal delivery of electrons under low UV fluence. Zhang et al. reported that bacterial cellular structure remained intact at a 300 mJ/cm^2 UV dose using the PMA-qPCR method (Zhang et al., 2015). In the current study when the UV exposure time was increased to 28 min (200 mJ/cm^2), bacterial respiratory activity was inhibited to some extent, except in *S. aureus* (Fig. 3A). According to principles of UV sterilization, an increase in UV irradiation time leads to the formation of more pyrimidine dimers on bacterial genomic DNA (Oguma et al., 2001), which may inhibit the transcription and translation of enzymes involved in respiration. For *S. aureus*, the Gram-positive bacterium contains thick peptidoglycan cell walls that provide increased rigidity to resist UV disinfection (Bouhdid et al., 2009).

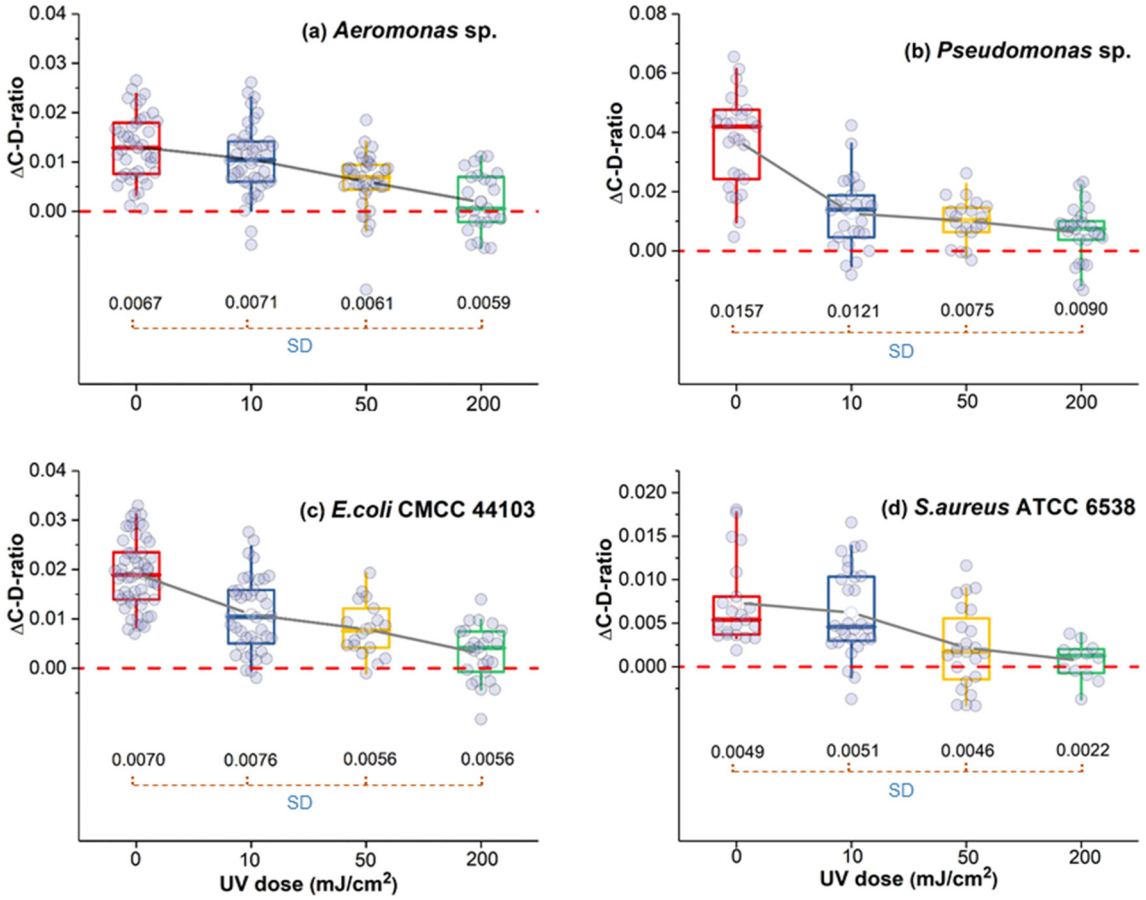

Fig. 6. The ΔC-D ratio of the four strains incubated for 1 h in D_2O-containing medium after treatment with different UV doses. Each dot represents a single cell. The area below the dashed red line shows cells in a state of metabolic "silence." The gray line connecting boxes connects the average ΔC-D ratio in each population under different UV doses. SD represents the standard deviation (SD) in ΔC-D ratios of individual cells in a given population. SD is another potential parameter for quantitatively evaluating and tracking the heterogeneity of bacterial metabolic activity under different UV doses. (For interpretation of the references to color in this figure legend, the reader is referred to the web version of this article.)

4.3. D_2O-labeled Raman method revealed the overall activity of VBNC bacteria

Compared with traditional methods, the rapid and nondestructive D_2O-labeling method tested in the current study enables reliable quantification of the metabolic activity of VBNC bacteria. The activities of all four bacterial strains remained at different levels after treatment with different UV fluences showing dose-dependent trends (Fig. 5). The mechanism of UV sterilization involves the formation of cis-syn cyclobutane pyrimidine dimers on bacterial genomic DNA, which block DNA replication and RNA transcription (Oguma et al., 2001; Santos et al., 2013; Zhang et al., 2015). At a low UV dose (10 mJ/cm^2), the increasing C-D ratios detected by Raman spectroscopy demonstrated that VBNC bacteria were still undergoing macromolecular synthesis, and that assimilation was greater than dissimilation. It can be further concluded that the amount of pyrimidine dimer formed at this UV fluence did not inhibit VBNC bacterial material and energy storage capacity. At a high UV dose (200 mJ/cm^2), the C-D ratio reached saturation and plateaued at a low level, indicating that the metabolic activity of bacteria was inhibited by UV irradiation. The D_2O-labeled Raman method may identify the effects of UV irradiation on the ability of bacteria to absorb water and synthesize organic matter. Metabolic activity based on substrate uptake involves complex active pathways, including transcription, translation, energy dependence, and enzyme activity (Kell et al., 1998; Ye et al., 2019; Ye et al., 2017b). Therefore, D_2O-labeled Raman could be a good method to detect the overall physiological activity of bacteria.

As the UV dose increased, the metabolic activity of VBNC cells decreased (Fig. 5). However, it is worth noting that even at extremely high UV doses, the bacteria still maintained some metabolic activity. This maintenance of metabolic activity has practical significance in terms of environmental processes (nutrient cycling reactions) and human health (infectivity, pathogenicity) (Kell et al., 1998). For example, non-culturable cells of pathogens may be capable of expressing virulence factors, such as toxins and invasions, in response to exogenous stimuli (Rahman et al., 1996). Moreover, physiological activity is a prerequisite for VBNC bacterial resuscitation.

4.4. Heterogeneous distribution of metabolic activity provides an optimization strategy for the disinfection process

D_2O-labeled Raman method can characterize the metabolic activity of single cells (cytological assay), while most other methods can only characterize the average metabolic activity of cell populations (bulk assay). In this work, metabolic heterogeneity (Fig. 6) indicated that different VBNC cells induced by the same UV dose in a given population may exhibit different residual metabolic activity, which demonstrated the variable resistance of bacterial cells to UV irradiation.

Fig. S2 shows a schematic diagram of two populations (A & B) with different activity distributions. Populations A and B have the same average metabolic activity, but for population A, the metabolic activities of most bacteria are close to the average value and show a narrower distribution range than population B. Certain individual cells in population B have higher activity and may exhibit greater resistance to

harsh environments than those in population A, posing a greater risk to human health. For disinfection, dosing near the average activity value (green line) may achieve high sterilization efficiency (99%) for population A. However, this disinfection dose would not kill the bacteria with high activity in population B. The yellow line was determined based on the activity distribution of population B and is more likely to achieve a high disinfection efficiency in that population. For populations with broad activity ranges, like population B, the required disinfection dose is higher than the calculated dose based on average activity. Therefore, the distribution of metabolic activity in a population can help inform better estimates of effective disinfection dose. Using D_2O-labed Raman to detect the activity distribution of a population can help optimize the appropriate disinfection dose for a safer and more efficient water disinfection process.

5. Conclusions

This study verifies that UV disinfection can induce model strains and environmental opportunistic pathogens into a VBNC state. And even at high UV doses, the respiration activity of VBNC bacteria remained high and the activity of populations conformed to the logarithmic normal distribution. We conclude that CTC-FCM method is suitable for detecting the essential viability of bacteria. The D_2O-labeled Raman method was found to quantify the metabolic activity of VBNC bacteria on a single cell level rapidly and reliably. And significant heterogenic distribution of bacterial activity was also detected. The results indicate that the D_2O-labeled Raman method is suitable for characterizing the overall metabolic activity.

Declaration of Competing Interest

The authors declare no competing financial interests.

Acknowledgments

The authors wish to acknowledge the K.C. Wong Education Foundation, the Natural Science Foundation of China (grant nos. 51478450, 51678551, 51678552), the Science and Technology Project of Fujian Province (grant no. 2016Y0082), the Science and Technology Project of Xiamen (grant no. 3502Z20162003, 3502Z20171003), the National Key Research and Development Program of China-International Collaborative Project from the Ministry of Science and Technology (grant no. 2017YFE0107300), and the Young Talent Project of the Institute of Urban Environment CAS (grant no. IUEQN 201505).

Appendix A. Supplementary data

Supplementary data to this article can be found online at https://doi.org/10.1016/j.envint.2019.05.077.

References

Albrecht, A., Witzenberger, R., Bernzen, U., Jäckel, U., 2007. Detection of airborne microbes in a composting facility by cultivation based and cultivation-independent methods. Ann Agric Environ Med 14, 81–85.
Bedard, E., Charron, D., Lalancette, C., Deziel, E., Prevost, M., 2014. Recovery of Pseudomonas aeruginosa culturability following copper- and chlorine-induced stress. FEMS Microbiol. Lett. 356, 226–234.
Belosevic, M.C., Craik, S.A., Stafford, J.L., Neumann, N.F., Kruithof, J., Smith, D.W., 2001. Studies on the resistance/reactivation of Giardia muris cysts and Cryptosporidium parvum oocysts exposed to medium-pressure ultraviolet radiation. FEMS Microbiol. Lett. 204, 197–203.
Ben Said, M., Masahiro, O., Hassen, A., 2010. Detection of viable but non cultivable Escherichia coli after UV irradiation using a lytic Qbeta phage. Ann Microbiol 60, 121–127.
Berry, D., Mader, E., Lee, T.K., Woebken, D., Wang, Y., Zhu, D., Palatinszky, M., Schintlmeister, A., Schmid, M.C., Hanson, B.T., Shterzer, N., Mizrahi, I., Rauch, I., Decker, T., Bocklitz, T., Popp, J., Gibson, C.M., Fowler, P.W., Huang, W.E., Wagner, M., 2015. Tracking heavy water (D2O) incorporation for identifying and sorting active microbial cells. Proc. Natl. Acad. Sci. U. S. A. 112, E194–E203.
Bolton, J.R., Linden, K.G., 2003. Standardization of methods for fluence (UV dose) determination in bench-scale UV experiments. J. Environ. Eng. 129, 209–215.
Bouhdid, S., Abrini, J., Zhiri, A., Espuny, M.J., Manresa, A., 2009. Investigation of functional and morphological changes in Pseudomonas aeruginosa and Staphylococcus aureus cells induced by Origanum compactum essential oil. J. Appl. Microbiol. 106, 1558–1568.
Chang, J.C.H., Ossoff, S.F., Lobe, D.C., Dorfman, M.H., Dumais, C.M., Qualls, R.G., Johnson, J.D., 1985. UV inactivation of pathogenic and indicator microorganisms. Appl. Environ. Microbiol. 49, 1361–1365.
Chen, S., Li, X., Wang, Y., Zeng, J., Ye, C., Li, X., Guo, L., Zhang, S., Yu, X., 2018. Induction of Escherichia coli into a VBNC state through chlorination/chloramination and differences in characteristics of the bacterium between states. Water Res. 142, 279–288.
Cui, L., Yang, K., Li, H.Z., Zhang, H., Su, J.Q., Paraskevaidi, M., Martin, F.L., Ren, B., Zhu, Y.G., 2018. Functional single-cell approach to probing nitrogen-fixing bacteria in soil communities by resonance Raman spectroscopy with (15)N2 labeling. Anal. Chem. 90, 5082–5089.
Dietersdorfer, E., Kirschner, A., Schrammel, B., Ohradanova-Repic, A., Stockinger, H., Sommer, R., Walochnik, J., Cervero-Arago, S., 2018. Starved viable but non-culturable (VBNC) Legionella strains can infect and replicate in amoebae and human macrophages. Water Res. 141, 428–438.
Ge, J., Huang, G., Sun, X., Yin, H., Han, L., 2019. New insights into the kinetics of bacterial growth and decay in pig manure-wheat straw aerobic composting based on an optimized PMA-qPCR method. Microb. Biotechnol. 12, 502–514.
Guo, M., Huang, J., Hu, H., Liu, W., Yang, J., 2012. UV inactivation and characteristics after photoreactivation of Escherichia coli with plasmid: health safety concern about UV disinfection. Water Res. 46, 4031–4036.
Guo, M.T., Kong, C., 2019. Antibiotic resistant bacteria survived from UV disinfection: safety concerns on genes dissemination. Chemosphere 224, 827–832.
Hijnen, W.A., Beerendonk, E.F., Medema, G.J., 2006. Inactivation credit of UV radiation for viruses, bacteria and protozoan (oo)cysts in water: a review. Water Res. 40, 3–22.
Huai-Shu, Xu., Roberts, N., Singleton, F., Attwell, R., Grimes, D., Colwell, R., 1982. Survival and viability of nonculturable Escherichia coli and Vibrio cholerae in the estuarine and marine environment. Microb. Ecol. 8, 313–323.
Justice, N.B., Li, Z., Wang, Y., Spaudling, S.E., Mosier, A.C., Hettich, R.L., Pan, C., Banfield, J.F., 2014. (15)N- and (2)H proteomic stable isotope probing links nitrogen flow to archaeal heterotrophic activity. Environ. Microbiol. 16, 3224–3237.
Kell, D.B., Kaprelyants, A.S., Weichart, D.H., Harwood, C.R., Barer, M.R., 1998. Viability and activity in readily culturable bacteria: A review and discussion of the practical issues. Antonie Van Leeuwenhoek 73, 169–187.
Lee, O.M., Kim, H.Y., Park, W., Kim, T.H., Yu, S., 2015. A comparative study of disinfection efficiency and regrowth control of microorganism in secondary wastewater effluent using UV, ozone, and ionizing irradiation process. J. Hazard. Mater. 295, 201–208.
Lee, S., Bae, S., 2018. Molecular viability testing of viable but non-culturable bacteria induced by antibiotic exposure. Microb. Biotechnol. 11, 1008–1016.
Lin, H., Ye, C., Chen, S., Zhang, S., Yu, X., 2017. Viable but non-culturable E. coli induced by low level chlorination have higher persistence to antibiotics than their culturable counterparts. Environ. Pollut. 230, 242–249.
Lindback, T., Rottenberg, M.E., Roche, S.M., Rorvik, L.M., 2010. The ability to enter into an avirulent viable but non-culturable (VBNC) form is widespread among Listeria monocytogenes isolates from salmon, patients and environment. Vet. Res. 41, 8.
Liu, Y., Wang, C., Tyrrell, G., Li, X.F., 2010. Production of Shiga-like toxins in viable but nonculturable Escherichia coli O157:H7. Water Res. 44, 711–718.
Mamane-Gravetz, H., Linden, K.G., 2005. Relationship between physiochemical properties, aggregation and u.v. inactivation of isolated indigenous spores in water. J. Appl. Microbiol. 98, 351–363.
Mangiaterra, G., Amiri, M., Di Cesare, A., Pasquaroli, S., Manso, E., Cirilli, N., Citterio, B., Vignaroli, C., Biavasco, F., 2018. Detection of viable but non-culturable Pseudomonas aeruginosa in cystic fibrosis by qPCR: a validation study. BMC Infect. Dis. 18, 701.
Nocker, A., Sossa, K.E., Camper, A.K., 2007. Molecular monitoring of disinfection efficacy using propidium monoazide in combination with quantitative PCR. J. Microbiol. Methods 70, 252–260.
Oguma, K., Katayama, H., Mitani, H., Morita, S., Hirata, T., Ohgaki, S., 2001. Determination of pyrimidine dimers in Escherichia coli and Cryptosporidium parvum during UV light inactivation, photoreactivation, and dark repair. Appl. Environ. Microbiol. 67, 4630–4637.
Oliver, J.D., 2000. The public health significance of viable but nonculturable bacteria. In: Nonculturable Microorganisms in the Environment. ASM Press, Washington, DC, pp. 277–300.
Oliver, J.D., 2005. The viable but nonculturable state in bacteria. J. Microbiol. 43, 93–100.
Oliver, J.D., 2010. Recent findings on the viable but nonculturable state in pathogenic bacteria. FEMS Microbiol. Rev. 34, 415–425.
Orta de Velasquez, M.T., Yanez Noguez, I., Casasola Rodriguez, B., Roman Roman, P.I., 2017. Effects of ozone and chlorine disinfection on VBNC Helicobacter pylori by molecular techniques and FESEM images. Environ. Technol. 38, 744–753.
Pianetti, A., Battistelli, M., Barbieri, F., Bruscolini, F., Falcieri, E., Manti, A., Sabatini, L., Citterio, B., 2012. Changes in adhesion ability of Aeromonas hydrophila during long exposure to salt stress conditions. J. Appl. Microbiol. 113, 974–982.
Rahman, I., Shahamat, M., Kirchman, P.A., Russek-Cohen, E., Colwell, R.R., 1994. Methionine uptake and cytopathogenicity of viable but nonculturable Shigella dysenteriae type 1. Appl. Environ. Microbiol. 6, 3573–3578.
Rahman, I., Shahamat, M., Chowdhury, M.A.R., Colwell, R.R., 1996. Potential virulence of viable but nonculturable Shigella dysenteriae type 1. Appl. Environ. Microbiol. 62, 115–120.

Ramamurthy, T., Ghosh, A., Pazhani, G.P., Shinoda, S., 2014. Current perspectives on viable but non-culturable (VBNC) pathogenic bacteria. Front. Public Health 2, 1–9.
Santos, A.L., Oliveira, V., Baptista, I., Henriques, I., Gomes, N.C., Almeida, A., Correia, A., Cunha, A., 2013. Wavelength dependence of biological damage induced by UV radiation on bacteria. Arch. Microbiol. 195, 63–74.
Servais, P., Agogue, H., Courties, C., Joux, F., Lebaron, P., 2001. Are the actively respiring cells (CTC+) those responsible for bacterial production in aquatic environments. FEMS Microbiol. Ecol. 35, 171–179.
Smith, E.M., Giorgio, P.A., 2003. Low fractions of active bacteria in natural aquatic communities? Aquat. Microb. Ecol. 31, 203–208.
Smith, J.J., McFeters, G.A., 1997. Mechanisms of INT (2-(4-iodophenyl)-3-(4-nitrophenyl)-5-phenyl tetrazolium chloride), and CTC (5-cyano-2,3-ditolyl tetrazolium chloride) reduction in Escherichia coli K-12. J. Microbiol. Methods 29, 161–175.
Song, Y., Cui, L., Lopez, J.A.S., Xu, J., Zhu, Y.G., Thompson, I.P., Huang, W.E., 2017. Raman-Deuterium Isotope Probing for in-situ identification of antimicrobial resistant bacteria in Thames River. Sci. Rep. 7, 1–10.
Suzuki, M.T., Giovannoni, S.J., 1996. Bias caused by template annealing in the amplification of mixtures of 16S rRNA genes by PCR. Appl. Environ. Microbiol. 62, 625–630.
Tao, Y., Wang, Y., Huang, S., Zhu, P., Huang, W.E., Ling, J., Xu, J., 2017. Metabolic-activity-based assessment of antimicrobial effects by D2O-labeled single-cell Raman microspectroscopy. Anal. Chem. 89, 4108–4115.
Tholozan, J.L., Cappelier, J.M., Tissier, J.P., Delatter, G., Federighi, M., 1999. Physiological characterization of viable-but-nonculturable campylobacter jejuni cells. Appl. Environ. Microbiol. 65, 1110–1116.
Trevors, J.T., 2011. Viable but non-culturable (VBNC) bacteria: gene expression in planktonic and biofilm cells. J. Microbiol. Methods 86, 266–273.
Valentine, D.L., Sessions, A.L., Tyler, S.C., Chidthaisong, A., 2004. Hydrogen isotope fractionation during H 2/CO 2 acetogenesis: hydrogen utilization efficiency and the origin of lipid-bound hydrogen. Geobiology 2, 179–188.
Whitesides, M.D., Oliver, J.D., 1997. Resuscitation of Vibrio vulnificus from the viable but nonculturable state. Appl. Environ. Microbiol. 63, 1002–1005.
Wilkinson, M.G., 2018. Flow cytometry as a potential method of measuring bacterial viability in probiotic products: A review. Trends Food Sci. Technol. 78, 1–10.
Ye, S., Zeng, G., Wu, H., Zhang, C., Dai, J., Liang, J., Yu, J., Ren, X., Yi, H., Cheng, M., Zhang, C., 2017a. Biological technologies for the remediation of co-contaminated soil. Crit. Rev. Biotechnol. 37, 1062–1076.
Ye, S., Zeng, G., Wu, H., Zhang, C., Liang, J., Dai, J., Liu, Z., Xiong, W., Wan, J., Xu, P., Cheng, M., 2017b. Co-occurrence and interactions of pollutants, and their impacts on soil remediation—a review. Crit. Rev. Environ. Sci. Technol. 47, 1528–1553.
Ye, S., Zeng, G., Wu, H., Liang, J., Zhang, C., Dai, J., Xiong, W., Song, B., Wu, S., Yu, J., 2019. The effects of activated biochar addition on remediation efficiency of co-composting with contaminated wetland soil. Resour. Conserv. Recycl. 140, 278–285.
Zeng, B., Zhao, G., Cao, X., Yang, Z., Wang, C., Hou, L., 2013. Formation and resuscitation of viable but nonculturable Salmonella typhi. Biomed. Res. Int. 2013, 1–7.
Zhang, S., Ye, C., Lin, H., Lv, L., Yu, X., 2015. UV disinfection induces a VBNC state in Escherichia coli and Pseudomonas aeruginosa. Environ Sci Technol 49, 1721–1728.
Zhang, S., Guo, L., Yang, K., Zhang, Y., Ye, C., Chen, S., Yu, X., Huang, W., Cui, L., 2018. Induction of Escherichia coli into a VBNC state by continuous-flow UVC and subsequent changes in metabolic activity at the single-cell level. Front. Microbiol. 9, 1–11.
Zhang, X.N., Gillespieb, A.L., Sessions, A.L., 2009. Large D/H variations in bacterial lipids reflect central metabolic pathways. PNAS 106, 12580–12586.